A comparative study of the oxidative and reductive dissolution of magnetite in acidified $CuSO_4$–acetonitrile–H_2O and $CuCl_2$–NaCl–H_2O leach solutions

Z.-Y. LU, D. M. MUIR

School of Mathematical and Physical Sciences, Murdoch University, Murdoch, Western Australia 6150, Australia

The oxidative and reductive dissolution of magnetite in acidified aqueous acetonitrile and acidified aqueous NaCl solutions have been investigated by electrochemical methods and correlated with the proton activity in these fundamentally different solution systems. The results are compared with the rates of magnetite dissolution in the presence of copper(II) and copper(I).

Under anodic or oxidizing leach conditions magnetite forms a passive Fe_2O_3 film which inhibits reaction, but under cathodic or reducing leach conditions in the presence of copper(I), magnetite is believed to dissolve via $(FeOH)^+$ intermediate and reacts up to 600 times faster. The rate of dissolution of magnetite depends on its potential and the activity of the proton. The rate follows a Butler–Volmer relationship with a Tafel slope of 120–130 mV per decade and exhibits a proton reaction order between 0.85 and 1.0. After allowing for changes in proton activity there is no significant difference between the rate of dissolution of magnetite in the sulphate and chloride leach solutions and no discernable effect of the presence of acetonitrile in the mixed solvent system. Electrochemical studies and leaching studies in which the potential is controlled by the Cu(II)–Cu(I) couple are in good agreement and lead to a fundamental understanding of the optimum conditions required to leach copper selectively from a Cu–Fe_3O_4 calcine derived from the segregation roasting of chalcopyrite concentrates.

1. Introduction

The dissolution kinetics and electrochemistry of iron oxides have been the subject of detailed investigations for many hydrometallurgical processes [1–3]. In one particular double-roast process for treating chalcopyrite concentrates [4–6], magnetite together with metallic copper is one of the main components of the calcine. The dissolution of copper is readily achieved by leaching with acidified solutions of copper(II) in brine or aqueous acetonitrile solutions, but the dissolution of magnetite is variable and depends on the leach conditions. In chloride or acetonitrile-containing solutions, copper(I) is stabilized by the formation of $CuCl_2^-$ and $Cu(AN)_3^+$ complex ions, respectively, and copper(II) is an

oxidant comparable in potential to Fe(III) in water. Our previous studies have compared the fundamental electrochemistry and kinetics of dissolution of copper and nickel in these two leach solutions [7].

This work extends the study to compare the fundamental differences of these leach solutions on the dissolution of magnetite. Differences can be expected because of changes in potential of the copper leach solution, changes in the activity of the proton, complexation by Cl^- or SO_4^{2-}, or the presence of an organic solvent. The activity coefficient of the proton differs significantly in strong salt solutions and in mixed aqueous-organic solutions [8, 9] and varies according to the concentration of NaCl or acetonitrile. Furthermore, during the leaching of copper from the
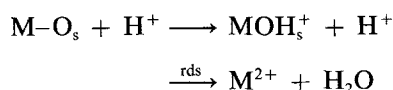
calcine, the solution potential typically changes from about 0.8 V to about 0.4 V versus standard hydrogen electrode (SHE) which are anodic and cathodic, respectively, of the rest potential of magnetite.

A number of studies have shown that the dissolution of magnetite in sulphuric acid [10, 11] and in perchloric acid [12] is accelerated under (chemical) reducing conditions or when a cathodic potential is applied to magnetite. This contrasts with the slow dissolution of magnetite in sulphuric acid under anodic conditions [13]. Besides the effect of potential, Valverde [3] has reported that certain inorganic and organic complexing agents also catalyse the dissolution of magnetite. He showed that the addition of Cl^- or Br^- enhanced the dissolution of various oxides in dilute $HClO_4$, and that the rate of dissolution in HCl varied according to the concentration of background NaCl. Recently, Bruyere and Blesa [14] showed an enhancement in the rate of magnetite dissolution in more concentrated H_2SO_4 solutions and interpreted this as due to anion complexation or exchange with HSO_4^- on a site-binding model in which the charge of the active site is determined by the relative abundance of $FeOH_2^+$ and $FeOH_2^+$ . . . X^- sites. However, in both these studies, no account was taken of the possible variation of the activity of the proton with the change in ionic strength of background salt.
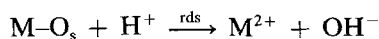
Electrochemical studies on magnetite corrosion in sulphuric acid [10] and in perchloric acid [12] have shown that, on applying an increasing cathodic potential, the corrosion current passes through a maximum with both the positive and negative branches of the peak exhibiting a Butler–Volmer relationship. According to the classic work of Vermilyea [15], oxides can behave under certain conditions as ideally reversible electrodes with their potential determined by H^+ and OH^- concentrations at the surface oxide sites. Freely dissolving crystals, like MgO, are predicted to show a decrease in their rate of dissolution upon applying large overpotentials because the rate of removal of the ion of opposite charge to the overpotential is impaired. Haruyama and Masamura [12] proposed that the positive branch of the cathodic peak was controlled by an anion

removal process, whilst the negative branch was controlled by the removal of Fe^{2+} from the mineral surface. However, Nicol [10] proposed that the reaction proceeds via FeO formation with no direct anion effect. He interpreted the decrease in current at high potentials as due to a passivating film of FeO formed on the electrode surface when the rate of formation of FeO exceeded its rate of dissolution by acid. Potentiodynamic and chronoamperometric studies by Allen et al. [16, 17] in more neutral perchlorate media, between pH 3 and pH 9, indicate that the current controlling reaction is the solid-state diffusion of the proton through the electrode. They proposed that the irreversible charge-transfer reaction is Fe(III) → Fe(II) in the lattice and that dissolution proceeds via $(FeOH)^+$ and removal of Fe^{2+} (aq) from the crystal surface.
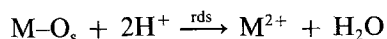
In general the rate is dependent on the pH or concentration of acid, but the exact order of reaction with respect to the proton and its mechanistic interpretation is open to debate. As discussed by Vermilyea [15], the order of reaction with respect to protons is indicative of the mechanism and rate determining step (rds) and can vary from 0.5 to 1.33 according to the ionic charge. For FeO dissolution the following mechanisms and proton reaction order apply:

$$M{-}O_s + H^+ \longrightarrow MOH_s^+ + H^+$$

$$\xrightarrow{\text{rds}} M^{2+} + H_2O$$

(proton order, 0.66)

$$M{-}O_s + H^+ \xrightarrow{\text{rds}} M^{2+} + OH^-$$

(proton order, 0.50)

$$M{-}O_s + 2H^+ \xrightarrow{\text{rds}} M^{2+} + H_2O$$

(proton order, 1.00)

However, without knowing the activity coefficients of the surface oxides and activated complex involved in the kinetic expression, it is difficult to interpret proton orders strictly.

From all this work it is clear that the potential and acid concentration determine the dissolution rate of magnetite, but the exact mechanism, the role of the anion and the order of the proton in the dissolution step are not well understood. A comparison of the electrochemistry

and dissolution kinetics of magnetite in acidified $CuCl_2$–$NaCl$–H_2O and $CuSO_4$–acetonitrile–H_2O leach solutions would clarify these aspects as well as establish optimum conditions for the selective leaching of copper from magnetite.

2. Experimental details

Both natural magnetite of high purity and synthetic magnetite were used for electrochemical and kinetic measurements. The synthetic magnetite was made from pure Fe_2O_3 powder produced by the reaction of $Fe(NO_3)_3$ solution with NH_4OH. After washing, drying and calcining, a stoichiometric amount of Fe_2O_3 powder was throughly mixed with iron powder to produce magnetite according to Reaction 1.

$$Fe + 4Fe_2O_3 \longrightarrow 3Fe_3O_4 \qquad (1)$$
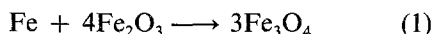
The size of both powders was minus 48 μm with an average size of about 5 μm. This mixed powder was moistened with about 1% water, then pressed into pellets at a pressure of 10^5 tonnes m^{-2}. The pellets were dried at $130°C$ to remove the moisture, and finally sintered at $1000°C$ under N_2 for more than 10 h in a tube furnace. X-ray diffraction analysis of the magnetite showed no evidence of Fe_2O_3 or iron, and showed sharp magnetite lines at the following d spaces (Å): 1.484 (m), 1.615 (m), 1.713 (w), 2.098 (m), 2.421 (w), 2.53 (s), 2.967 (s) and 4.85 (m). The crystal structure of both our natural magnetite and our synthetic magnetite had a density of about 4.7–$4.8\,g\,cm^{-3}$ (natural Fe_3O_4 = $5.2\,g\,cm^{-3}$). The pellets had a resistance of less than $0.5\,\Omega$. A low ohmic contact resistance was achieved by drilling and pressing a copper metal rod into the back of the electrode using silver epoxy paste to ensure even contact. The electrode was kept under pressure overnight as the epoxy was cured, then encased in a Teflon and epoxy holder in the usual way. It was noted that the resistance of the magnetite decreased with an increase of the sintering temperature. Because low resistance electrodes were obtained, the IR drop across the magnetite electrode was neglected. Both synthetic and natural magnetite showed identical electrochemical properties.

The instruments and cells used for the electrochemical and kinetic measurements were the same as reported previously [7]. The proton activities in all solutions were measured by using a standard hydrogen electrode. A saturated calomel electrode reference (SCE) was used in aqueous chloride solutions, whilst a mercurous sulphate reference electrode was used in aqueous acetonitrile–sulphate solutions. All potential measurements were corrected for liquid junction potential. For aqueous chloride solutions, the liquid junction potential was calculated by using the Henderson equation [18, 19]. For mixed acetonitrile–H_2O solutions, the liquid junction potentials derived by Senanayake [20] were applied.

3. Results and discussion

3.1. Cyclic voltammetry

Fig. 1 compares the cyclic voltammogram of synthetic magnetite in a solution of HCl containing 4 M Cl^- and in H_2SO_4 containing 4 M acetonitrile, with the cyclic voltammogram of 0.05 M Fe(II) on platinum.

It can be seen that magnetite displayed a well-defined cathodic reduction peak around 0.25 V versus SHE and a broad ill-defined oxidation current quite unlike the redox reactions of Fe(III) and Fe(II) on platinum.

In solutions of high HCl and H_2SO_4 concentrations (Fig. 1b, c) a variation in the rotation speed of the magnetite electrode had only a small effect on the current density. This indicated that the reaction was solid-state electrochemically controlled rather than solution diffusion-controlled. Furthermore, the current peak potentials obtained by scanning in the anodic and cathodic directions were the same in both the chloride and sulphate solutions. Variation of the potential scan rate, v, produced a well-defined change in peak current, i_p, in 0.1 M HCl solutions with $i_p \propto v^{1/2}$. However, in 1 M HCl and 1 M H_2SO_4 the increase in i_p with v was not so well defined or reproducible. The square-root relationship between i_p and v is predicted by the Sevcik equation [21] for a diffusion-controlled current flowing across an electrode as a consequence of an irreversible process. Such a relationship was observed by Allen *et al.* [16, 17] in their studies on magnetite dissolution at pH 3
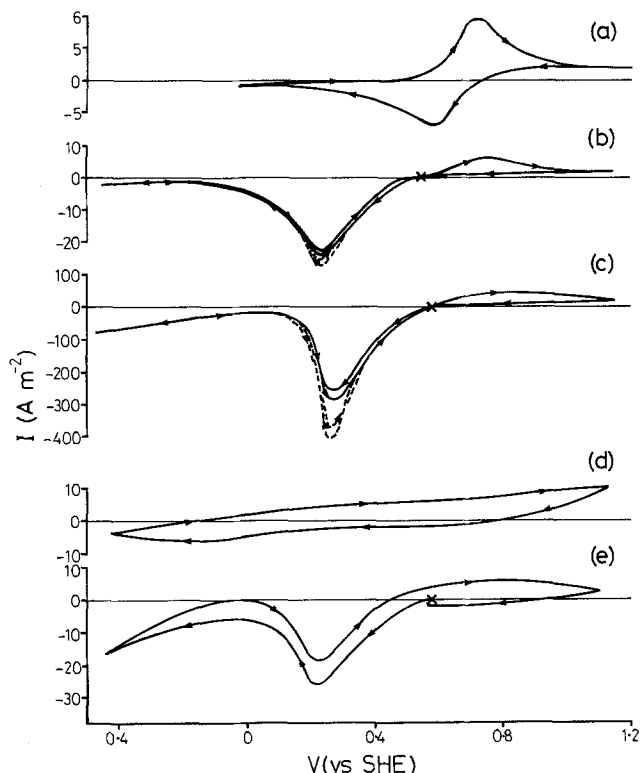
Fig. 1. Cyclic voltammogram of Fe_3O_4 compared with Fe(II) on platinum. (a) Platinum in 0.05 M Fe(II), 0.1 M HCl, 4 M NaCl, quiescent. (b) Fe_3O_4 in 1 M H_2SO_4, 4 M acetonitrile, quiescent (solid lines) and 1000 r.p.m. (dashed lines). (c) Fe_3O_4 in 1 M HCl, 3 M NaCl, quiescent (solid lines) and 1000 r.p.m. (dashed lines). (d) Fe_3O_4 in 0.01 M HCl, 4 M NaCl, quiescent. (e) As (d), 1000 r.p.m. All measured at 25° C and 5 mV s^{-1} with calomel or mercurous sulphate reference electrodes.

to pH 7. At low acid concentrations (0.01 M HCl) in this work, the cathodic current peak was less well defined (Fig. 1d, e), but was now dependent on the rotation speed due to limited proton diffusion, as predicted by the Levich equation [22].

3.2. Dissolution of magnetite under cathodic conditions

Detailed studies on the effect of stirring on the dissolution of a rotating disc of magnetite held at various constant cathodic potentials confirmed the insensitivity of the reaction to proton mass transport under the conditions of high acidity. As shown by Fig. 2, there was only a small change in the cathodic current with $\omega^{1/2}$ in the presence of 1 M HCl when magnetite was held at either the cathodic peak potential of 0.05 V versus SCE or at a potential of 0.02 V, commonly attained in copper leach solutions containing excess Cu(I). A notable dependence on stirring was observed in 0.01 M HCl at the cathodic peak potential (Fig. 2), but not at either −0.20 V or 0.20 V (the region of the negative and positive branches of the cathodic peak)

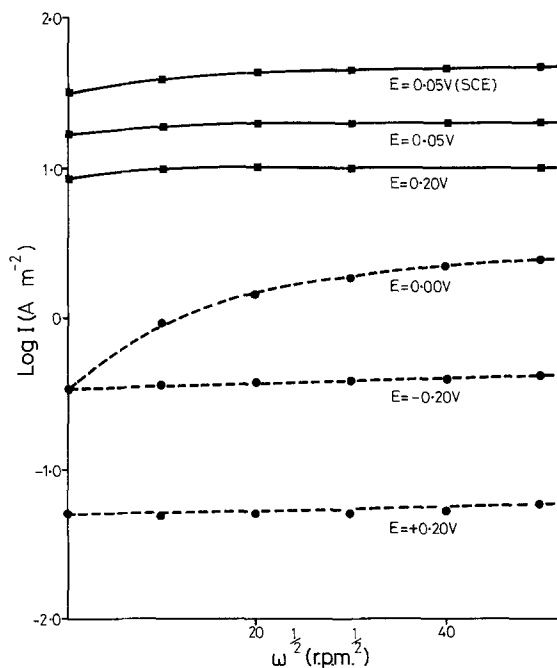Fig. 2. Effect of stirring on the dissolution of a magnetite disc held at different cathodic potentials in 0.01 M HCl–4 M NaCl and 1.0 M HCl–3 M NaCl solutions at 25° C. Solid lines, 1.0 M HCl–3 M NaCl; dashed lines, 0.1 M HCl–4 M NaCl.

Table 1. Current efficiency of the cathodic dissolution of Fe_3O_4 (25° C, 400 r.p.m.)

Electrolyte (M)		Applied constant current		Iron dissolved $(10^{-5}\ mol\,m^{-2}\,s^{-1})$	Current efficiency according to Equation 2
NaCl or acetonitrile	HCl or H_2SO_4[a]	Current density $(A\,m^{-2})$	Coulombs (passed in 30 min)		
4	0.02	0	Natural dissolution	< 0.02	
3.9	0.1	0		0.18 ± 0.05	
3	1	0		0.32 ± 0.03	
2	2	0		0.08 ± 0.03	
4	0.02	2.0	0.18	3.1	100
4	0.02	10.0	0.90	16.2	104
4	0.02	15.0	1.35	22.6	97
3.9	0.1	2.0	0.18	2.9	95
3.9	0.1	10.0	0.90	15	97
3.9	0.1	15.0	1.35	23	100
3.0	1.0	10.0	0.90	15.9	102
3.0	1.0	35.0	3.15	56.0	103
3.0	1.0	100.0	9.0	159	102
3.0	1.0	300.0	27.0	476	102
6[a]	1[a]	50.0	4.5	76	98
6[a]	1[a]	100.0	9.0	160	101

[a]As acetonitrile + H_2SO_4.

when the cathodic current was an order of magnitude lower.

Under constant current electrolysis at potentials within the positive branch of the magnetite cathodic reduction peak, the dissolution of iron in the various acidified chloride and sulphate electrolytes of interest had a coulombic efficiency of 100% and followed the stoichiometry of Equation 2, as first proposed by Engell [11] and in agreement with that previously reported in perchloric acid [12].

$$Fe_3O_4 + 8H^+ + 2e \longrightarrow 3Fe^{2+} + 4H_2O \quad (2)$$
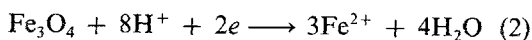
The results given in Table 1 show that the natural dissolution rate of magnetite is very low compared to that when even low current densities are applied. There was no evidence of passivation in 1 M HCl or 1 M H_2SO_4 even at high current densities around $100\,A\,m^{-2}$.

Fig. 3 shows the potentiodynamic polarization curves for magnetite in aqueous chloride and aqueous acetonitrile–sulphate solutions. From these curves the measured Tafel slope of the positive branch of the curves is between 120–130 mV per decade whilst the slope of the

negative branch lies between 200–300 mV per decade. The similarity in the current–potential relationships in the chloride and sulphate supports the view by Nicol [10] that the reaction is lattice-dependent and not affected by any specific complexation or adsorption of Cl^- or SO_4^{2-}, or by adsorption of acetonitrile onto the magnetite surface. Greater differences could be expected if the rate was controlled by an anion removal step. However, there is clearly a difference in the effect of acid concentration on the rate of leaching in these two solution systems which requires analysis in terms of the activity of the proton.

3.3. Effect of acid concentration and proton activity

The non-oxidative dissolution of metal sulphides and oxides in acid solution is sometimes dependent on the acid concentration [10], but several authors have shown reactions which more closely follow the proton activity in solution [23–25]. Nicol [10] interprets the apparent success of the two approaches to the nature of the transition
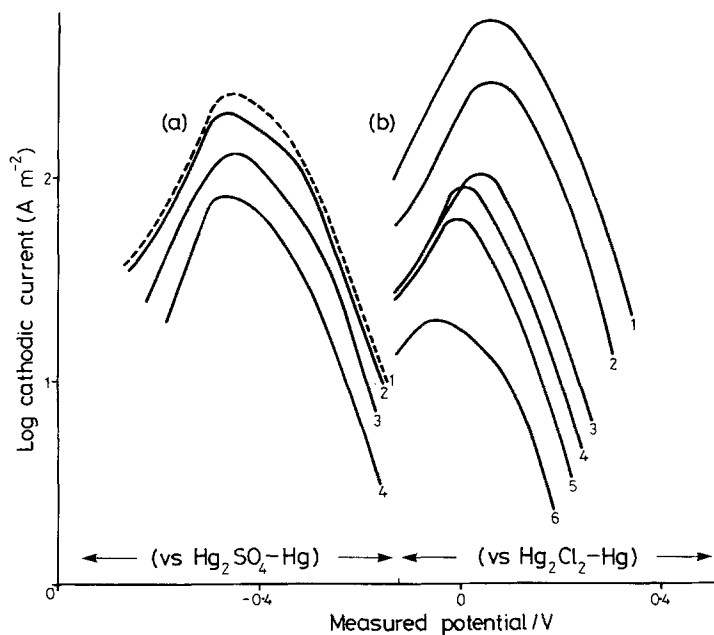
Fig. 3. Comparison of the effect of acid concentration and potential on the dissolution rate of a magnetite rotating disc in (a) acetonitrile–sulphate and (b) chloride solutions at 25° C; 5 mV s^{-1}; 400 r.p.m. (a) 1: 1 M H_2SO_4–H_2O. 2: 1 M H_2SO_4–6 M acetonitrile. 3: 0.5 M H_2SO_4–6 M acetonitrile. 4: 0.5 M H_2SO_4–6 M acetonitrile. (b) 1: 2 M HCl–2 M NaCl. 2: 1 M HCl–1 M NaCl. 3: 0.1 M HCl–4 M NaCl. 4: 0.1 M HCl–2 M NaCl. 5: 0.1 M HCl–0.5 M NaCl. 6: 0.01 M–4 M NaCl.

state and the rate determining step. A comparison of the rate of magnetite dissolution in NaCl and acetonitrile–H_2O solutions clearly shows significant differences at the same acid concentration (Fig. 3). But an analysis of the different effects of these solutions on the activity of the proton should resolve whether these differences are due to anion effect, solvent effect or changes in proton activity.

Majima and Awakura [24] and Jansz [26] have demonstrated that the activity of the proton rises significantly with addition of NaCl and increasing ionic strength due to a decrease in the activity of free water in solution. According to the hydration theory for strong electrolyte solutions [26], the single-ion activity of the proton is directly dependent on the free water activity and the hydration number of the proton. Measurements of the rate of dissolution of magnetite by 0.1 M HCl indeed show a steady increase when the concentration of NaCl is increased (Fig. 3b, curves 3–5). By contrast, the activity coefficient of the proton in mixed solvent systems often passes through a minimum as organic solvent is added to water, due to changes in the water basicity and solvent structure [27]. In acetonitrile–H_2O mixtures the activity coefficient of the proton in perchloric acid solutions decreases to about 0.3 in 50 mol % acetonitrile

relative to that in pure water, then rises sharply as the organic concentration increases further [28]. However, in acetonitrile–H_2O mixtures containing sulphuric acid, the changes in activity with solvent are more complex due to the buffering by sulphate ion and changes in the sulphate–bisulphate equilibrium.

Precise measurements of the proton activity in various HCl–NaCl and $HClO_4$–NaCl solutions were carried out using a SHE relative to a SCE reference and a saturated 3.5 M KCl salt bridge. Potentials were corrected for liquid junction potential using the Henderson equation [18, 19], and the calculated proton activities are reported in Table 2.

At constant ionic strength (4 M) the activity coefficient of HCl in various HCl–NaCl mixtures remained around 4.2; however, when the ionic strength was increased by addition of either $HClO_4$ to 4 M NaCl or NaCl to 0.1 M HCl, the activity coefficient of the proton increased. There was nearly a fivefold increase in proton activity (a_{H+}) when 4 M NaCl is added to 0.1 M HCl (Table 2).

Similar measurements in H_2SO_4–acetonitrile–H_2O solutions are subject to large liquid junction potentials which vary according to the bridge electrolyte, solvent composition and background acid concentration. Liquid junc-

Table 2. Proton activities (a_{H+}) in HCl and $HClO_4$ solutions containing NaCl at 25° C

Solution [NaCl] (M)	4 M (NaCl + HCl)		4 M NaCl + $HClO_4$		0.1 M HCl + NaCl	
	[HCl] (M)	a_{H+}	$[HClO_4]$ (M)	a_{H+}	[NaCl] (M)	a_{H+}
3.99	0.01	0.043	0.01	0.052	0	0.093
3.95	0.05	—	0.05	0.261	0.5	0.109
3.90	0.10	0.42	0.10	0.52	1.0	0.122
3.50	0.50	2.01	0.50	3.2	2.0	0.167
3.00	1.00	4.14	1.00	8.3	3.0	0.266
2.00	2.00	8.40	2.00	—	3.9	0.420

tion potentials are minimized with a 3.5 M $NaClO_4$ salt bridge and can be determined for each solvent mixture by measurements on standard cells and electrolytes [20]. The measured proton activities of 0.1 M H_2SO_4 in water containing between 2 and 10 M acetonitrile and the corresponding liquid junction potentials (E_j) are reported in Table 3, which shows that the proton activity in 1 M H_2SO_4 solution decreased from about 1.53 to about 1.26 on addition of up to 10 M acetonitrile. There was a small increase in γ_{H+} in 6 M acetonitrile solutions when the concentration of H_2SO_4 was increased from 0.1 to 1.0 M. However, it should be noted that the liquid junction potential in 6 M acetonitrile solution varied from -4 to $+4$ mV over this range of sulphuric acid concentration and was subject to error from changes in SO_4^{2-}/HSO_4^- ratio at the bridge junction. It is not possible to be as precise on proton activities in sulphate media as in chloride media, where liquid junction potentials are smaller and more predictable.

To establish the dependence of magnetite dissolution rate on proton activities, currents were measured at various applied potentials in the same HCl–NaCl and H_2SO_4–acetonitrile solutions and correlated with a_{H+} values. Fig. 4 shows there is a good correlation and straight line relationship between log i and log a_{H+}, in both sulphate and chloride media with slopes, ∂ log i/∂ log a_{H+}, ranging from 0.84 to 1.06. Within the limits of accuracy of the activity and current measurements there did not appear to be any significant difference between the SO_4^{2-} and Cl^- system, despite known differences in ion pairing or complexation of these anions with Fe^{2+}, nor any effect of acetonitrile on the rate of dissolution of magnetite. The measured slopes compared favourably with a slope of 1.0 predicted from the Butler–Volmer equation and Reactions 3–6 outlined in the following mechanism. The proposed reaction mechanism for magnetite dissolution under cathodic conditions [10] involves reduction of Fe(III) to Fe(II) in the

Table 3. Effect of acetonitrile and H_2SO_4 concentration on proton activity as measured by e.m.f. at 25° C

[Acetonitrile] (M)	$[H_2SO_4]$ (M)	e.m.f.	E_j(Henderson) (mV)	E_j(Solvation) (mV)	E_{corr} (mV)	a_{H+}
0	1.0	-247	-14	0	-233	1.37
2	1.0	-234	-14	10	-230	1.53
6	1.0	-237	-14	10	-233	1.37
10	1.0	-233	-14	16	-235	1.26
6	0.1	-298	-6	10	-302	0.093
6	0.5	-250	-12	10	-248	0.76
6	1.0	-237	-14	10	-233	1.37
0	0.1	-308	-6	0	-302	0.093
0	0.5	-267	-12	0	-255	0.58
0	1.0	-247	-14	0	-233	1.37

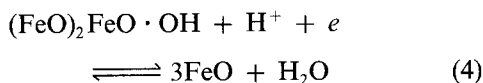Cell: Hydrogen | test ‖ 3.5 M $NaClO_4$ ‖ 3.5 M NaCl ‖ calomel.
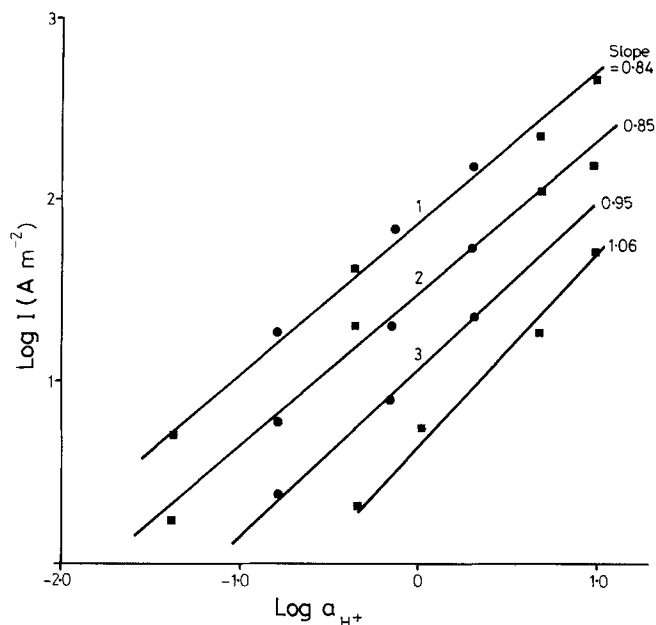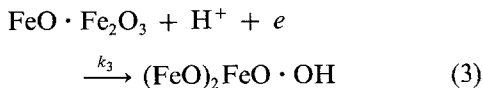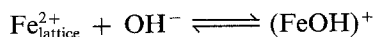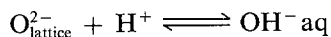
Fig. 4. Correlation between cathodic current of magnetite at various potentials with proton activities in chloride and acetonitrile–sulphate solutions at 25° C. ■, 4 M (NaCl + HCl); ●, 6 M acetonitrile; 1, 0.15 V; 2, 0.20 V; 3, 0.25 V; 4, 0.30 V (SCE).

lattice (Equations 3 and 4) followed by non-oxidative dissolution of FeO and desorption of Fe(II)aq from the surface (Equations 5 and 6):

$$FeO \cdot Fe_2O_3 + H^+ + e$$

$$\xrightarrow{k_3} (FeO)_2FeO \cdot OH \qquad (3)$$

$$(FeO)_2FeO \cdot OH + H^+ + e$$

$$\rightleftharpoons 3FeO + H_2O \qquad (4)$$

$$3FeO + 3H^+ \rightleftharpoons 3Fe(OH)^+\,ads \qquad (5)$$

$$3Fe(OH)^+\,ads + 3H^+$$

$$\rightleftharpoons 3Fe(II)aq + 3H_2O \qquad (6)$$

At higher pH [16, 17]

$$O^{2-}_{lattice} + H^+ \rightleftharpoons OH^-aq$$

$$Fe^{2+}_{lattice} + OH^- \rightleftharpoons (FeOH)^+$$
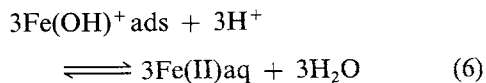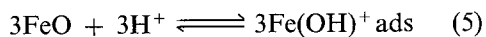
According to this mechanism, the rate of Reaction 3 should be governed by the Butler–Volmer expression (Equation 7) and will be the rate-determining step at low overpotentials (ΔE)

$$i = nFk_3 a_{H^+} \exp{(\alpha z F\Delta E/RT)} \qquad (7)$$

Thus, under chemical leaching conditions the dissolution should depend on both the solution potential and the concentration of the reduced species, like Cu(I), undergoing electron transfer.

Indeed, the recent work of Bruyere and Blesa [14] demonstrated the acceleration of magnetite dissolution in 1 M H_2SO_4 by addition of Fe(II). It also follows from Equation 7 that the Tafel slope $\partial\Delta E/\Delta \log i$ will be 118 mV at 25° C if $\alpha = 0.5$, and that the current will be directly proportional to the proton activity, as indeed was closely found by our experiments.

At moderate overpotentials towards the cathodic peak potential, Reaction 3 becomes rate determining. On the other hand the desorption of Fe(II)aq from the surface (Reaction 6) becomes the controlling factor at high over-potentials when there is sufficiently high acid concentrations to avoid proton transport control.

3.4. Anodic dissolution of magnetite

Under anodic conditions, magnetite quickly passivates and the dissolution of magnetite in 0.5 M H_2SO_4 solution containing 6 M acetonitrile is very slow. Chronopotentiometric measurements at four different current densities (Fig. 5) show a rapid rise in potential to over 1.2 V within a few seconds of the current being applied. Oxygen is then evolved from the surface. After 30 min, no more than 2×10^{-7} M iron(III) was detected in solution for each of the current
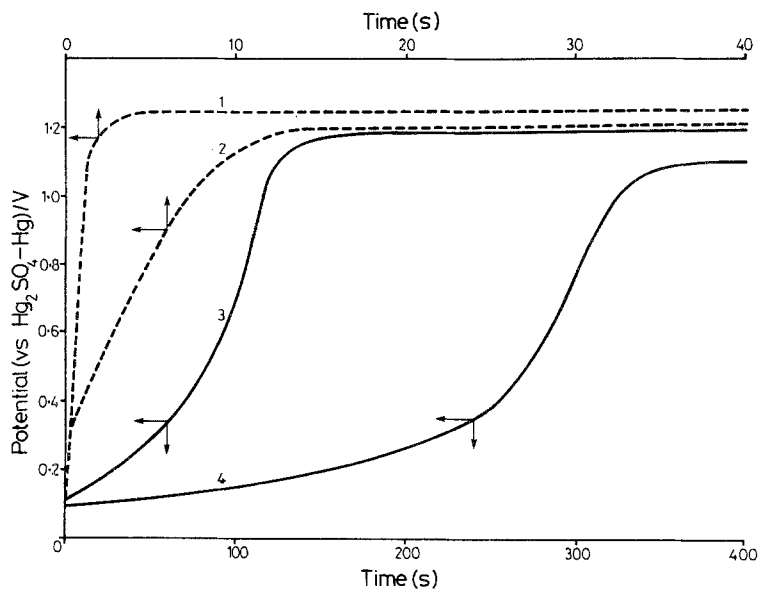
Fig. 5. Passivation of magnetite with time at various anodic current densities in 0.5 M H_2SO_4 containing 6 M acetonitrile at 25° C. 1, 50 A m^{-2}; 2, 20 A m^{-2}; 3, 5 A m^{-2}; 4, 2 A m^{-2}.

densities. Presumably, in contrast to FeO, the electrochemical reaction is the formation of a non-conducting passive film of Fe_2O_3 (Equation 8), which is very slowly attacked by acid (Equation 9).

$$2Fe_3O_4 + H_2O - 2e \longrightarrow 3Fe_2O_3 + 2H^+ \quad (8)$$

$$3Fe_2O_3 + 18H^+ \longrightarrow 6Fe(III) + 9H_2O \quad (9)$$
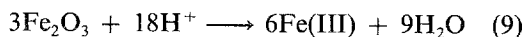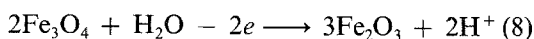
Using values for the electrode area and the coulombs passed through the electrode before the plateau potential was reached, the thickness of the Fe_2O_3 film required to passivate the surface was estimated to be about 0.1 μm.

Interrupted chronoamperometric studies on magnetite in 0.5 M H_2SO_4 containing 6 M acetonitrile under both anodic and cathodic potential conditions highlight the differences in the reactivity of the FeO and Fe_2O_3 films formed. As shown in Fig. 6a, at a potential of -0.4 V (versus $Hg–Hg_2SO_4$) in the region of the positive branch of the cathodic peak, there was only a small decay in current after switching on; after a short interruption the effect was reproduced exactly. Similar results were obtained at potentials in the region of the negative branch of the cathodic peak (Fig. 6b, c) except that the decay in current with time was much more pronounced, reflecting the greater extent of FeO film formation in this region. By contrast, inter-

rupted electrolysis in the anodic region (Fig. 6d) showed both significant current decay after switching on, and only partial restoration of the current after switching off for 60 s.

3.5. Dissolution of magnetite in copper (II) leach solutions

In a practical leaching process in which the mixed copper–magnetite calcine is leached with copper(II) chloride in aqueous sodium chloride, or with copper(II) sulphate in aqueous acetonitrile, the redox potential changes from values positive of the rest potential of magnetite (approximately 0.6 V versus SHE at 25° C) to values negative of the rest potential. Therefore the dissolution of magnetite is governed by the acid concentration and the mixed potential, as shown schematically by the Evans diagram (Fig. 7). This diagram superimposes the individual current–potential curves of magnetite and the Cu(II)–Cu(I) couple measured on platinum. Whilst it is acknowledged that the rate of oxidation of Cu(I) or reduction of Cu(II) on magnetite may not be the same as that on platinum, similar rates and I–V curves may be expected, so that the diagram can be used to describe qualitatively the leaching reaction and known results. The diagram shows that during the initial leaching of copper with Cu(II), the dissolution of
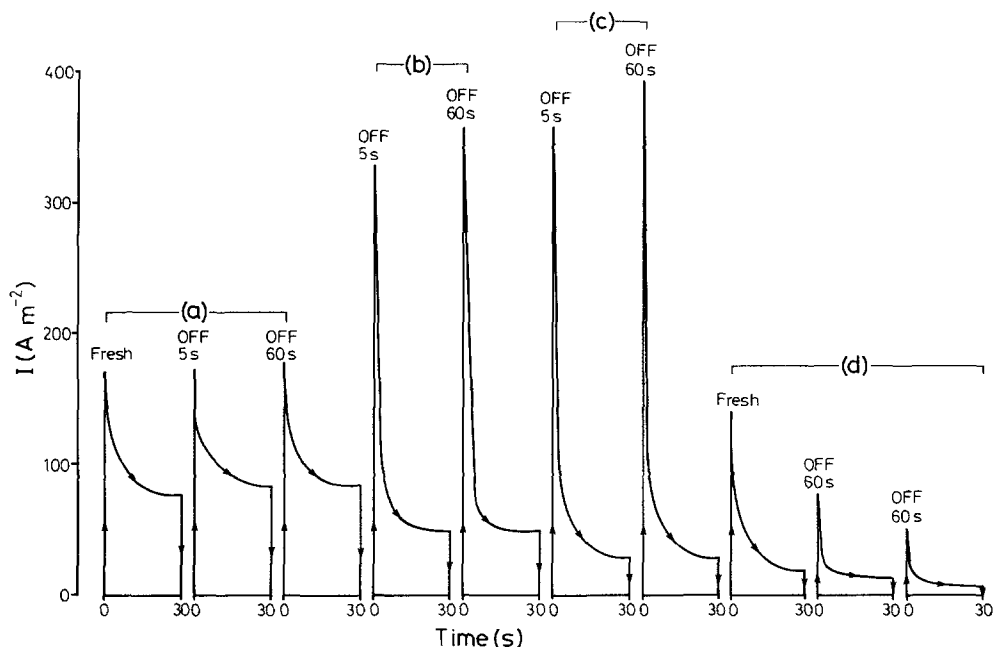
Fig. 6. Interrupted electrolysis of Fe_3O_4 in 0.5 M H_2SO_4 containing 6 M acetonitrile at different cathodic and anodic potentials. (a) -0.4 V; (b) -0.6 V; (c) -0.8 V; (d) $+0.6$ V (reference Hg_2SO_4–Hg). Temperature, 25°. C.

magnetite is under anodic control, but as the concentration of Cu(II) falls and Cu(I) increases, the dissolution comes under cathodic control. However, under the normal range of leaching conditions the mixed potential does not extend to the cathodic peak potential of magnetite.

Thus, under all practical leach conditions the dissolution of magnetite is directly dependent on proton activity.

Measurements of the rate of dissolution of magnetite in 1 M HCl–3 M NaCl solutions (in which the potential was changed by suitable
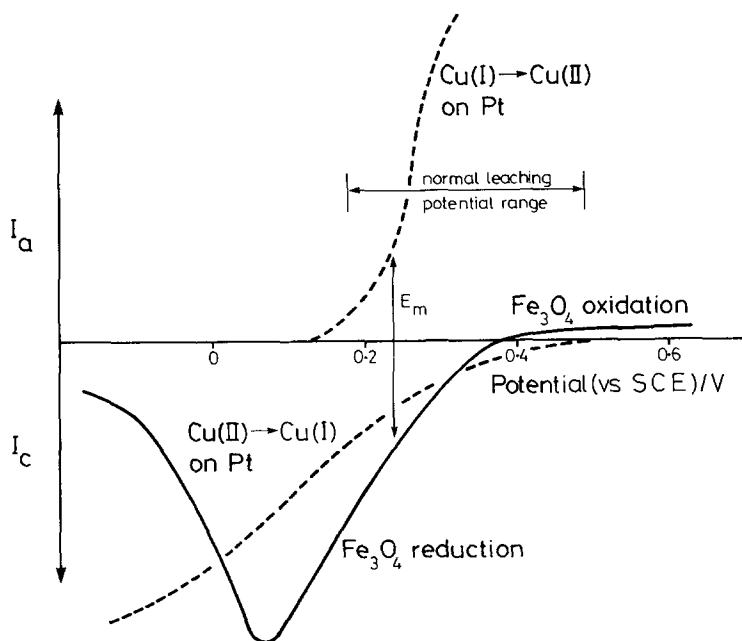

Fig. 7. Schematic Evans diagram for the leaching of Fe_3O_4 in acidified Cu(II)–Cu(I) solutions.

Table 4. *Effect of solution potential on the rate of dissolution of magnetite disc in HCl–NaCl containing various $Cu(II)$–$Cu(I)$ ratios*

Copper in solution	Measured potential[a] (V versus SCE)	Dissolution rate[b] (10^{-5} mol Fe m^{-2} s^{-1})
0.1 M Cu(II)	0.46–0.51	0.16
No copper	0.42–0.45	0.32
0.2 M Cu(I) + Cu(II)	0.39–0.41	2.1
0.2 M Cu(I) + Cu(II)	0.36	4.5
0.2 M Cu(I) + Cu(II)	0.34	7.5 (≤ 11[c])
0.2 M Cu(I) + Cu(II)	0.315	13 (14[c])
0.2 M Cu(I)	0.24	107 (110[c])

[a] Measured on Fe_3O_4 electrode.
[b] Measured by AAS at 400 r.p.m. at 25° C.
[c] Measured electrochemically at same applied potential.

addition of Cu(II) or Cu(I)), and the dissolution monitored by chemical analysis of iron in solution, compared well with the expectation from electrochemical studies (Table 4). The table shows that magnetite dissolves 600 times faster in 1 M HCl containing 0.1 M Cu(I) than in the same acid solution containing 0.1 M Cu(II). Further studies on the effect of HCl concentration at constant ionic strength confirmed that the dissolution rate was directly dependent on acid concentration and proton activity and was largely unaffected by stirring (Table 5). These leach tests also confirmed that it was the solution potential, the presence of copper(I) and the acid concentration that dictated the rate. Rates in 1 M H_2SO_4 solution were slightly slower than in 2 M HCl in accord with the previously observed lower proton activity and smaller corrosion currents in sulphuric acid media.

4. Conclusions

Electrochemical studies have indicated that the rate-determining step in magnetite dissolution is the reduction of Fe(III) to Fe(II) in the lattice which is controlled by the potential and activity of the proton in solution. In strongly acidic solutions the dissolution is basically unaffected by stirring and is governed by the electrochemical kinetics of the reduction step. For practical applications such as the selective leaching of copper from magnetite using $CuCl_2$–NaCl–H_2O or $CuSO_4$–acetonitrile–H_2O, it makes little difference which leach system is chosen provided due attention is given to Eh and pH control. It is of interest to compare magnetite reactivity in these acidified leach solutions because of the fundamental difference in proton activity in brine and mixed solvent solutions. Copper can

Table 5. *Effect of acid concentration, copper (I) and stirring rate on the dissolution of magnetite disc in NaCl and acetonitrile–H_2O solutions*

Solution (M)			Solution potential (V versus SCE)	Dissolution rate (10^{-5} mol Fe m^{-2} s^{-1})		
[Cl$^-$ or acetonitrile]	[Cu(I)]	[H$^+$]		100 r.p.m.	400 r.p.m.	1600 r.p.m.
3.9[a]	0.1	0.1[c]	0.24	8.9	9.3	9.6
3.0[a]	0.1	1.0[c]	0.24	104	107	111
2.0[a]	–	2.0[c]	0.45	0.77	–	0.80
6.0[b]	–	2.0[d]	–0.10[e]	0.5	–	0.5

[a] As NaCl; [b] as acetonitrile; [c] as HCl; [d] as H_2SO_4; [e] reference, Hg_2SO_4–Hg.

be leached selectively at high pH with vigorous stirring, or at low pH by maintaining oxidizing conditions with respect to the rest potential of magnetite.

Acknowledgements

References

[1]   I. H. Warren and M. G. Hay, *Trans. Inst. Min. Metall.* **84** (1975) C49.

[2]   J. J. Byerley, G. L. Rempel and G. F. Garrido, *Hydrometallurgy* **4** (1979) 317.

[3]   N. Valverde, *Physik Chem.* **80** (1976) 333.

[4]   Z. -Lu, E. J. Grimsey and A. J. Parker, *Proc. Australas. Inst. Min. Metall.* **288** (1983) 19.

[5]   Z.-Y. Lu, E. J. Grimsey and D. M. Muir, 'Proceedings Chemeca '85 Conference', Inst. Chem. Eng., Perth, W. Australia (1985) p. 169.

[6]   A. J. Parker, D. M. Muir, Y. C. Smart and J. Avraamides, *Hydrometallurgy* **7** (1981) 213.

[7]   Z.-Y. Lu, D. M. Muir and I. M. Ritchie, *J. Electroanal. Chem.* **168** (1984) 163.

[8]   D. M. Muir and G. Senanayake, in 'Extractive Metallurgy '85' (edited by M. J. Jones), IMM, London (1985) p. 65.

[9]   D. M. Muir and A. J. Parker, in 'Hydrometallurgy: Research Development and Plant Practice' (edited by K. Osseo-Asare and J. D. Miller), AIME, New York (1982) p. 341.

[10] M. J. Nicol, in 'Hydrometallurgy: Research Development and Plant Practice' (edited by K. Osseo-Asare and J. D. Miller), AIME, New York (1982) p. 177.

[11] H. J. Engell, *Z. Physik. Chem. NF.* **7** (1956) 158.

[12] S. Haruyama and K. Masamura, *Corros. Sci.* **18** (1978) 263.

[13] V. M. Novukovskii and Yu. A. Likhachev, *Zashch. Metal.* **7** (1971) 514 (Russ.)

[14] V. I. E. Bruyere and M. A. Blesa, *J. Electroanal. Chem.* **182** (1985) 141.

[15] D. A. Vermilyea, *J. Electrochem. Soc.* **113** (1966) 1067.

[16] P. D. Allen, N. A. Hampson and G. J. Bignold, *J. Electroanal. Chem.* **99** (1979) 299.

[17] *Idem, ibid.*, **111** (1980) 223.

[18] P. Z. Henderson, *Z. Phys. Chem.* **59** (1907) 118.

[19] *Idem, ibid.*, **63** (1908) 325.

[20] G. Senanayake, PhD Thesis, Murdoch University (1986).

[21] A. Sevcik, *Collect. Czech. Chem. Commun.* **12** (1948) 349.

[22] V. G. Levich 'Physicochemical Hydrodynamics', Prentice-Hall, Englewood Cliffs, NJ (1962).

[23] H. Majima, Y. Awakura and T. Mishima, *Metall. Trans.* **16B** (1985) 23.

[24] H. Majima and Y. Awakura, *ibid.* **12B** (1981) 141.

[25] H. Majima, Y. Awakura and N. Misaki, *ibid.* **12B** (1981) 645.

[26] J. J. C. Jansz, *Hydrometallurgy* **11** (1983) 13.

[27] R. H. Boyd, in 'Acidity Functions in Solute–Solvent Interactions' (edited by J. F. Coetzee and C. D. Ritchie), Marcel Dekker, New York (1969).

[28] D. M. Muir and M. C. Whiting, *J.C.S. Perkin II* (1975) 1316.